THE JOURNAL OF PHYSICAL CHEMISTRY Letters

Letter

pubs.acs.org/JPCL

Strain-Induced Segregation in Bimetallic Multiply Twinned Particles

Lingxuan Peng,[†] Richard P. Van Duyne,[‡] and Laurence D. Marks*[,†]

[†]Department of Materials Science and Engineering and [‡]Department of Chemistry, Northwestern University, Evanston, Illinois 60208, United States

Supporting Information

ABSTRACT: We analyze the possibility of strain-induced segregation in bimetallic multiply twinned particles by an analytic first-order expansion within a continuum model. The results indicate that while the change in free energy may be small, there will be a noticeable segregation of larger atoms to the external surface and smaller ones to the core, which could have interesting effects when such nanoparticles are used as heterogeneous catalysts.

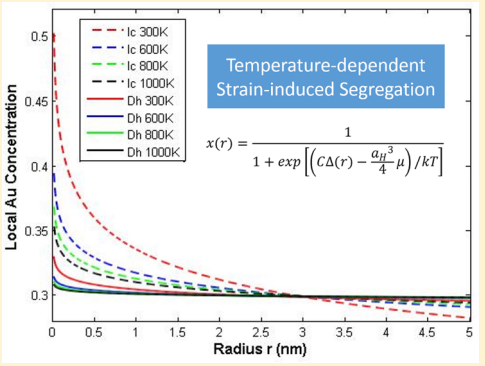

Bimetallic nanoparticles have received substantial attention in recent years. A considerable number of experimental and theoretical studies have shown that their unique optical,[1−3] electrical,[3,4] and catalytic[5−7] properties not only depend on size[8−11] but also the composition distribution in the bimetallic nanoparticles.[2,3,12] The structures of bimetallic nanoparticles are more complicated due to their one additional degree of freedom—composition. They can be phase separated, such as in core−shell[13,14] and Janus[15,16] structures, or alloys where the two elements are randomly mixed.[17−19]

Many numerical simulation approaches, such as density functional theory (DFT), Monte Carlo simulation using empirical/semiempirical potentials including second-moment approximation tight binding (SMATB) potentials, and embedded atom potentials (EAM) have been used to analyze the segregation of alloy nanoparticles with fixed shapes for a limited number of atoms.[20−28] Regardless of the empirical potential or the particle structure approximation, the pure numerical calculations can be very accurate for specific cases, but it is hard to impossible in most cases to extract the trends as a function of composition, temperature, size, and other parameters. Here, analytical models are more powerful. For instance, an analytical alloy Wulff construction model developed by Ringe et al.[29] to predict the surface segregation and equilibrium shape of single-crystalline bimetallic nanoparticles using thermodynamics as a function of composition showed the importance of a bulk starvation energy that arises when atoms segregate to the surface, something that was otherwise not apparent. For completeness, we note that this model was only for one temperature, a point that we will return to later.

In many cases, nanoparticles are not single crystals but instead multiply twinned particles (MTPs) containing twin boundaries with the decahedral MTPs (Dh) containing 5 single-crystal segments and the icosahedral MTPs (Ic) containing 20. In both cases, the single-crystal segments are not completely space-filling; therefore, there are some internal distortions present.[30,31] These internal strains have been considered in several ways. Bagley[32] and Yang[33] were the first to suggest a structure transformation from face-centered cubic (FCC) to body-centered orthorhombic structure, but this view is no longer considered to be correct. While the leading strain term is the homogeneous strain as first analyzed by Ino,[34] the proper description for both is via classic Volterra disclinations[35] as first pointed out by de Wit.[30] Marks, Howie, and Yoffe[36] further analyzed the inhomogeneous strain in both decahedral and icosahedral particles, giving an approximate solution for the latter. More recent finite element analysis (FEA) calculation by Patala et al.[37] has shown the nonuniform elastic strain distribution in decahedral particles, something also recently seen in larger-scale molecular dynamics calculations[38] as well as earlier atomistic papers.[39] While the hypothesis that there could be segregation and/or impurities connected to the large strains in MTPs exists in the unpublished literature, to our knowledge, there has not been any detailed analytical analysis of this to date.

In this Letter, we show that elastic strains induce segregation inside of bimetallic MTPs and derive an analytic solution of the composition distribution in thermal equilibrium. We also show that the degree of segregation depends on strain, temperature, as well as the homogeneous concentration.

To start, we need to briefly describe the strain in MTPs, which drives segregation. Considering first the Dh, after joining

Received: April 6, 2015
Accepted: May 5, 2015

DOI: 10.1021/acs.jpclett.5b00706
J. Phys. Chem. Lett. 2015, 6, 1930−1934

the five single-crystalline units together along a [110] axis, a positive wedge disclination with a 7°20′ solid angle deficiency is created. The plane-strain solution for a Dh treated as a cylinder was first given by de Wit,[30] which is used as an approximation in this note. The strains in cylindrical coordinates are

$$e_{rr} = \left[\frac{1-2\nu}{2(1-\nu)}\right]\varepsilon_D\left[\ln\left(\frac{r}{R}\right)+1\right] - \frac{\varepsilon_D}{2} \quad (1)$$

$$e_{\varphi\varphi} = \left[\frac{1-2\nu}{2(1-\nu)}\right]\varepsilon_D \ln\left(\frac{r}{R}\right) + \frac{\varepsilon_D}{2} \quad (2)$$

where υ is the Poisson's ratio, r is the 2D radial vector, R is the radius of the Dh, and ε_D is the strain of the Dh, which is 0.0205.[31]

For an Ic, the particle can be approximated as an elastic sphere with radial distortions. An approximation for the strains by Yoffe, Howie, and Marks in spherical coordinates is[31]

$$e_{rr} = \frac{2}{3}\varepsilon_I\left(\frac{1-2\nu}{1-\nu}\right)\left[\ln\left(\frac{r}{R}\right)+1\right] - \frac{2\varepsilon_I}{3} \quad (3)$$

$$e_{\theta\theta} = e_{\varphi\varphi} = \frac{2}{3}\varepsilon_I\left(\frac{1-2\nu}{1-\nu}\right)\ln\left(\frac{r}{R}\right) + \frac{\varepsilon_I}{3} \quad (4)$$

where r is the 3D radial position, R is the radius of the Ic, and ε_I is the strain of the Ic, which is 0.0615.[31]

Patala et al.[37] recently computed the elastic strain energy using FEA for Dh and Ic and compared them with the these approximations.[31] The strain energy of Dh is approximately 0.75 times the plane strain result, and for Ic, it is about 1.45 times that of eqs 3 and 4.

We consider here the case where the local bulk concentration in a bimetallic MTP varies as a function of position r. A first-order perturbation approximation is used, which assumes that the local strain from the disclination does not change, and there is an additional energy term arising from a local expansion or contraction as any segregation is assumed to be equivalent to a local lattice expansion or contraction. Cottrell and Bilby (1949) used the same approximation to estimate the energy change arising from interstitial carbon solute atoms around a dislocation line in α-iron.[40] The change in strain energy is then

$$E^{\text{strain}} = -K\int \Delta\cdot\frac{(a(C_i)^3 - {a_H}^3)}{{a_H}^3}\,dV \quad (5)$$

where K is the bulk modulus, Δ the cubic dilatation, C_i the local concentration of element i, $a(C_i)$ the local lattice parameter, a_H the lattice parameter at the homogeneous concentration and $(a(C_i)^3 - {a_H}^3)/{a_H}^3$ the local expansion or contraction. This change in energy term is analogous to a PdV term.

For a binary system, segregation also changes the configurational entropy, $\Delta S_{mix} = S_{seg} - S_o$, where S_{seg} is the configurational entropy after segregation and S_o the entropy before segregation, that is, the entropy of the solid solution when the composition is homogeneous. We assume that the bimetallic system is an ideal binary solid solution; hence, the change in free energy from the entropy of mixing is

$$E^{\text{Entropy}} = \int nkT\{x(r)\ln x(r) + (1-x(r))\ln(1-x(r)) - [C_H \ln C_H + (1-C_H)\ln(1-C_H)]\}/{a_H}^3\,dV \quad (6)$$

where n is the number of atoms in a unit cell, which is 4 for FCC metals, $x(r)$ is the local concentration of element i, and C_H is the homogeneous bulk concentration of element i.

The total change in energy is the sum $E = E^{\text{Strain}} + E^{\text{Entropy}}$, which is a function of position r and the local bulk concentration $x(r)$. To obtain the most stable configuration, we minimize the total change in energy $E(r,x)$ with respect to $x(r)$, which is solved by a calculus of variation method (see the Supporting Information).

The solution for the local bulk concentration has a Fermi–Dirac-like distribution

$$x(r) = \frac{1}{1+\exp\left[\left(C\Delta(r) - \frac{{a_H}^3}{4}\mu\right)/kT\right]} \quad (7)$$

where k is Boltzmann's constant; $C = -(3K/4){a_j}^2(a_i - a_j)$, which is a constant; and μ is the chemical potential of species i, which can be solved numerically by applying a mass conservation constraint. The composition distribution of element i is analogous to the distribution of point defects around a dislocation line (Cottrell atmosphere),[40] caused by the elastic strain field around the dislocation; see also ref 41 for a more recent overview.

Of course, in many cases, the solid solution of two metals is not ideal, that is, the interactions between i–i, j–j, and i–j are not identical. A regular solution model can be considered by adding an additional enthalpy of mixing term, $\Omega x(r)(1-x(r))$, where Ω can be either positive or negative, depending on the systems. By introducing this term into the calculations, no simple analytical solution can be obtained, and the composition profile has to be calculated numerically. A detailed derivation is given in the Supporting Information. Here, we present a system-independent analytical solution of the simplest possible ideal solution model in order to investigate the general trends.

The assumption that the local strain remains constant is only valid for systems that have two elements with small lattice mismatch. The lattice parameter for Au and Ag are 4.0782 and 4.0853 Å, respectively, and they have a lattice mismatch of 0.17%. Therefore, the Ag–Au alloy case will be used as an example here.

The bulk modulus and Poisson's ratio used for Au–Ag alloys with different Au homogeneous concentration are obtained by fitting the elastic modulus at different Au concentrations[42] for the Au–Ag alloy from the literature with a quadratic function. The elastic modulus and the fitted plot for the bulk modulus and Poisson's ratio are provided in the Supporting Information. It is noted that the elastic modulus has a slight increase of 5–10% when the particle is small,[43] which could be added as an additional size-dependent term. The lattice parameters are assumed to vary linearly between Au and Ag.

In Figure 1, we calculated the total change in energy as well as the contributions from both the strain and entropy of mixing as a function of Au homogeneous concentration for a Dh with a radius of 5 nm and a thickness of 3 nm at 300 and 1000K, respectively. The total energy change is small. The entropy of mixing always favors mixing of atoms; therefore, the segregation inside of a particle always results in an increase of free energy, neglecting the strain term. However, the change in strain energy from segregation dominates, and the net change in energy is negative at thermal equilibrium. As the temperature increases, the energy contribution from the entropy of mixing increases linearly with absolute temperature T (in Kelvin),

DOI: 10.1021/acs.jpclett.5b00706
J. Phys. Chem. Lett. 2015, 6, 1930–1934

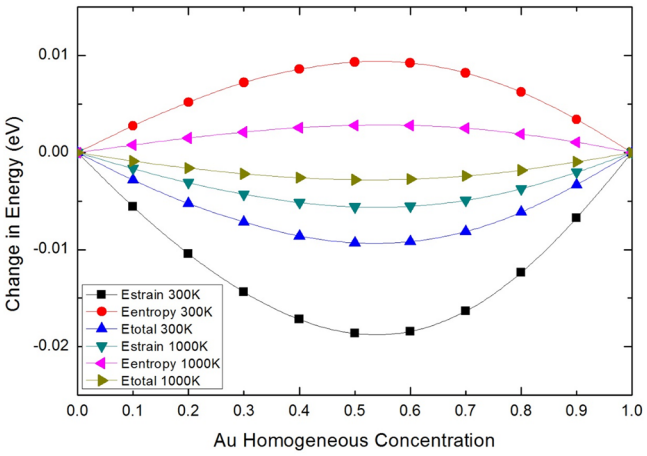

Figure 1. Change in energy of a Dh (5 nm in radius, 3 nm in thickness) as a function of homogeneous (initial) Au concentration at different temperatures.

ignoring differential thermal expansion. As a result, the segregation is less significant at higher temperature.

In contrast to the energy change, the compositional change may be significant, as shown in Figure 2, for the strain-induced

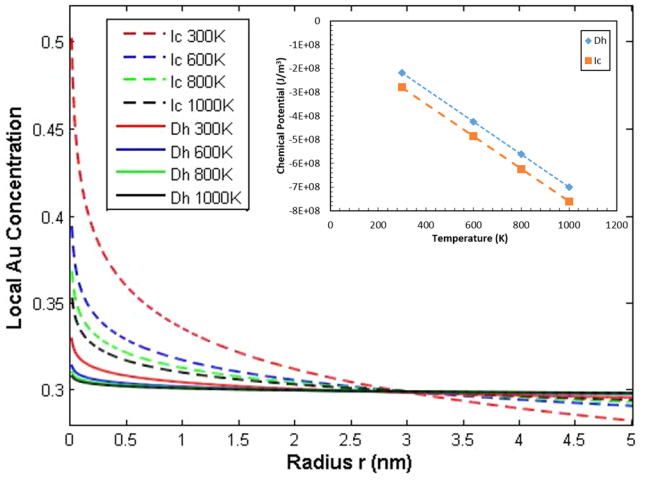

Figure 2. Temperature-dependent segregation inside of Dh and Ic bimetallic nanoparticles. The local Au concentration is plotted as a function of radius, where 0 represents the center of the particle. Dh particles (5 nm in radius with 3 nm thickness) are estimated as an elastic cylinder that only has plane strain. Ic particles (5 nm in radius) are estimated as an elastic sphere that has radial strains.

segregation in Dh and Ic with a Au homogeneous concentration of 0.3 at different temperatures as well as chemical potentials. The chemical potentials of Au as a function of homogeneous Au concentration at various temperatures were calculated and are included in the Supporting Information. The elastic strain energy in Ic is 1 order of magnitude larger than the elastic strain energy in Dh. As a consequence, the segregation in Ic is more significant than the segregation in Dh.

To illustrate the degree of Au segregation inside of a MTP, the variance of local Au concentration was taken and integrated over the whole particle; the degree of Au segregation is expressed as the square root of the ratio between the integrated variance and the total volume of the MTP as

$$\mathrm{Deg}_{\mathrm{Seg}} = \sqrt{\frac{\int (x(r) - C_{\mathrm{H}})^2 \, \mathrm{d}V}{\int \mathrm{d}V}} \tag{8}$$

In Figure 3, the degrees of segregation at high temperature (1000 K) and room temperature (300 K) as a function of Au

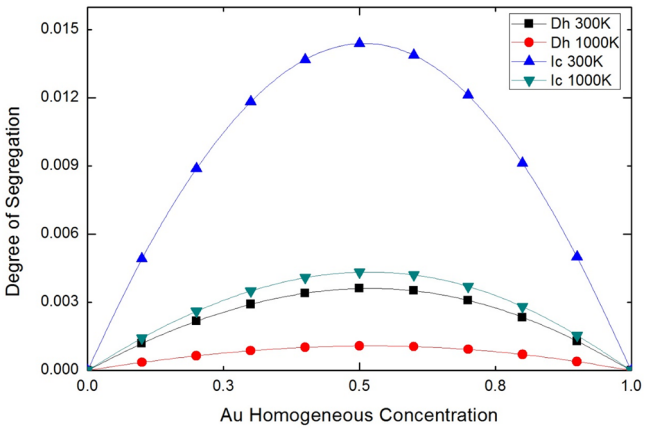

Figure 3. Degree of segregation of Dh and Ic as a function of the Au homogeneous concentration at different temperatures. The degree of segregation is linearly related to the change in energy in a particle. Ic has higher inhomogeneous strains in the particle, which results in a higher degree of segregation.

homogeneous concentration for Dh (r = 5 nm, thickness = 3 nm) and Ic (r = 5 nm) are compared. The degree of segregation is proportional to the change in energy from the segregation.

The elastic strain fields in bimetallic MTPs drive atoms with a smaller lattice parameter to segregate toward the center of the particles and larger atoms to the surface, therefore creating inhomogeneities inside of bimetallic MTPs. At low temperature, the segregation is more significant; at higher temperature, the contribution from the entropy of mixing drives the bulk composition toward homogeneity. It is straightforward that temperature will have a similar effect on segregation to surfaces both within an alloy Wulff construction[29] or with MTPs. Ic, with higher solid angle deficiency, have a higher degree of segregation than Dh particles.

There is some experimental evidence in support of the analysis above. High-resolution electron microscopy studies have been used to target understanding the segregation behavior in bimetallic nanoparticles with different shapes or structures at the atomic scale.[18,44−47] Some recent experimental studies of Fe−Pt Ic nanoparticles have shown that Pt segregates toward the surface,[48,49] consistent with our prediction; other work for Dh has not observed segregation.[50] For completeness, it should be mentioned that there can also be ordered phases in these particles where the ordered phase is thermodynamically more stable at certain composition ratios. For instance, $L1_0$ ordered structures were observed via high-angle annular dark field (HAADF) aberration-corrected STEM in both single-crystal and multiply twinned FePt particles after annealing,[50,51] consistent with DFT[52] and Monte Carlo[53,54] calculations. These $L1_0$ ordered structures are formed at high temperature, usually via a postannealing process,[51,55] when we predict segregation effects to be minimal. In the above analysis, the alloy phase was assumed to be the most stable phase, which is not always the case. More work is needed.

DOI: 10.1021/acs.jpclett.5b00706
J. Phys. Chem. Lett. 2015, 6, 1930−1934

It also should be noted that there are other well-known factors that affect segregation in bimetallic MTPs, such as surface energies, size, or charge-transfer-induced ordering.[56,57] For the case of Au−Ag, the surface energy change from surface segregation is approximately 100 eV for a 5 nm Dh, which is around 4 orders of magnitude larger than the energy gain from the strain-induced segregation in the bulk (Figure 1). For the Ic case, the energy change from strain-induced segregation is around 50 times larger than the case in Dh, which is due to the higher degree of strain and segregation in an Ic. As shown in eq 5, the strain energy scales as the cube of the size mismatch and therefore could be a much larger energy contribution in some cases; for instance, there are known to be some interesting ordering phenomena in PtFe Dh particles that are related to stress-relief.[50,52] For systems with a large surface energy difference, the surface-energy-driven segregation will dominate, but if they are similar, the strain-induced segregation could be substantial. For instance, in large lattice mismatch alloys, the stress-driven segregation will dominate if the surface energies are comparable.

To our knowledge, there are no experimental data yet for a dominant role for stress-relief-driven segregation in disordered alloys in the thermodynamic stability of MTPs, but we would not be surprised if there exist cases where it will occur. Independent of the energy change, there is still noticeable segregation taking place, especially in Ics, and this could have a large effect upon the chemical behavior.

For the large size difference limit, a related phenomenon has been observed in numerical calculations[58−60] that represents an extreme limit of segregation. Here, phase separation can occur with the larger atoms on the outside where the stresses are tensile and the smaller ones on the inside where the stresses are compressive. While these calculations were for the alloys AgNi, AgCu, and AgCo, which do not form a continuous solid solution, it is not impossible that the extreme limit of segregation to a core−shell structure could occur in miscible alloys.

There are some very interesting implications for bimetallic catalysts because strain-induced segregation can either promote or reduce surface segregation. As mentioned above, besides systems with small lattice mismatches, such as Pt−Pd, which follows the formulation derived above, there are many possible combinations. For instance, for Ag−Pd and Ni−Pt, where there are larger differences in the atomic radii, the change in strain energy will be large, which results in a large change in the free energy and the strain-induced segregation being more pronounced. We will pose the possibility of designing novel catalysts to exploit this segregation as an interesting line of future research.

■ ASSOCIATED CONTENT

Supporting Information

Detailed derivation of the bulk concentration profile in bimetallic MTPs, determination of the bulk modulus and Poisson's ratio for a Au−Ag alloy, and chemical potential of decahedral and icosahedral Au−Ag alloy nanoparticles at different temperatures. The Supporting Information is available free of charge on the ACS Publications website at DOI: 10.1021/acs.jpclett.5b00706.

■ AUTHOR INFORMATION

Corresponding Author

*E-mail: l-marks@northwestern.edu.

Notes

The authors declare no competing financial interest.

■ ACKNOWLEDGMENTS

This work was supported by the Materials Research Center (MRSEC) at Northwestern University. MRSEC (DMR-1121262) is funded through the National Science Foundation.

■ REFERENCES

(1) Wilcoxon, J. Optical Absorption Properties of Dispersed Gold and Silver Alloy Nanoparticles. *J. Phys. Chem. B* **2009**, *113*, 2647−56.
(2) Motl, N. E.; Ewusi-Annan, E.; Sines, I. T.; Jensen, L.; Schaak, R. E. Au−Cu Alloy Nanoparticles with Tunable Compositions and Plasmonic Properties: Experimental Determination of Composition and Correlation with Theory. *J. Phys. Chem. C* **2010**, *114*, 19263−19269.
(3) Link, S.; Wang, Z. L.; El-Sayed, M. A. Alloy Formation of Gold−Silver Nanoparticles and the Dependence of the Plasmon Absorption on Their Composition. *J. Phys. Chem. B* **1999**, *103*, 3529−3533.
(4) Drube, W.; Treusch, R.; Sham, T. K.; Bzowski, A.; Soldatov, A. V. Sublifetime-Resolution Ag L_3-Edge XANES Studies of Ag−Au Alloys. *Phys. Rev. B* **1998**, *58*, 6871−6876.
(5) Bracey, C. L.; Ellis, P. R.; Hutchings, G. J. Application of Copper−Gold Alloys in Catalysis: Current Status and Future Perspectives. *Chem. Soc. Rev.* **2009**, *38*, 2231−43.
(6) Wang, C.; Yin, H. G.; Chan, R.; Peng, S.; Dai, S.; Sun, S. H. One-Pot Synthesis of Oleylamine Coated AuAg Alloy NPs and Their Catalysis for CO Oxidation. *Chem. Mater.* **2009**, *21*, 433−435.
(7) Sinfelt, J. H. Catalysis by Alloys and Bimetallic Clusters. *Acc. Chem. Res.* **1977**, *10*, 15−20.
(8) Chen, H.; Kou, X.; Yang, Z.; Ni, W.; Wang, J. Shape- and Size-Dependent Refractive Index Sensitivity of Gold Nanoparticles. *Langmuir* **2008**, *24*, 5233−7.
(9) Henry, A. I.; Bingham, J. M.; Ringe, E.; Marks, L. D.; Schatz, G. C.; Van Duyne, R. P. Correlated Structure and Optical Property Studies of Plasmonic Nanoparticles. *J. Phys. Chem. C* **2011**, *115*, 9291−9305.
(10) Ringe, E.; Van Duyne, R. P.; Marks, L. D. Correlated Structure−Optical Properties Studies of Plasmonic Nanoparticles. *J. Phys. Conf. Ser.* **2014**, *522*, 012006.
(11) Ringe, E.; Langille, M. R.; Sohn, K.; Zhang, J.; Huang, J. X.; Mirkin, C. A.; Van Duyne, R. P.; Marks, L. D. Plasmon Length: A Universal Parameter to Describe Size Effects in Gold Nanoparticles. *J. Phys. Chem. Lett.* **2012**, *3*, 1479−1483.
(12) Suntivich, J.; Xu, Z.; Carlton, C. E.; Kim, J.; Han, B.; Lee, S. W.; Bonnet, N.; Marzari, N.; Allard, L. F.; Gasteiger, H. A.; Hamad-Schifferli, K.; Shao-Horn, Y. Surface Composition Tuning of Au−Pt Bimetallic Nanoparticles for Enhanced Carbon Monoxide and Methanol Electro-Oxidation. *J. Am. Chem. Soc.* **2013**, *135*, 7985−91.
(13) Lu, J.; Low, K. B.; Lei, Y.; Libera, J. A.; Nicholls, A.; Stair, P. C.; Elam, J. W. Toward Atomically-Precise Synthesis of Supported Bimetallic Nanoparticles Using Atomic Layer Deposition. *Nat. Commun.* **2014**, *5*, 3264.
(14) Serpell, C. J.; Cookson, J.; Ozkaya, D.; Beer, P. D. Core@Shell Bimetallic Nanoparticle Synthesis via Anion Coordination. *Nat. Chem.* **2011**, *3*, 478−83.
(15) Langlois, C.; Li, Z. L.; Yuan, J.; Alloyeau, D.; Nelayah, J.; Bochicchio, D.; Ferrando, R.; Ricolleau, C. Transition from Core−Shell to Janus Chemical Configuration for Bimetallic Nanoparticles. *Nanoscale* **2012**, *4*, 3381−8.
(16) Song, Y.; Liu, K.; Chen, S. AgAu Bimetallic Janus Nanoparticles and Their Electrocatalytic Activity for Oxygen Reduction in Alkaline Media. *Langmuir* **2012**, *28*, 17143−17152.
(17) Herzing, A. A.; Watanabe, M.; Edwards, J. K.; Conte, M.; Tang, Z. R.; Hutchings, G. J.; Kiely, C. J. Energy Dispersive X-ray Spectroscopy of Bimetallic Nanoparticles in an Aberration Corrected Scanning Transmission Electron Microscope. *Faraday. Discuss.* **2008**, *138*, 337−351 ; discussion 421−434..

DOI: 10.1021/acs.jpclett.5b00706
J. Phys. Chem. Lett. 2015, 6, 1930−1934

(18) Cui, C. H.; Gan, L.; Heggen, M.; Rudi, S.; Strasser, P. Compositional Segregation in Shaped Pt Alloy Nanoparticles and Their Structural Behaviour during Electrocatalysis. *Nat. Mater.* **2013**, *12*, 765−771.
(19) Chen, S.; Ferreira, P. J.; Shao-Horn, Y. Surface Segregation in Pt_3Co Nanoparticles Characterized by Scanning Transmission Electron Microscopy. *Microsc. Microanal.* **2007**, *13*, 604−605.
(20) Baskes, M. I. Modified Embedded-Atom Potentials for Cubic Materials and Impurities. *Phys. Rev. B: Condens. Matter Mater. Phys.* **1992**, *46*, 2727−2742.
(21) Cleri, F.; Rosato, V. V. Tight-Binding Potentials for Transition Metals and Alloys. *Phys. Rev. B: Condens. Matter Mater. Phys.* **1993**, *48*, 22−33.
(22) Rosato, V.; Guillope, M.; Legrand, B. Thermodynamical and Structural Properties of f.c.c. Transition Metals Using a Simple Tight-Binding Model. *Philos. Mag. A* **1989**, *59*, 321−336.
(23) Daw, M. S.; Baskes, M. I. Embedded-Atom Method — Derivation and Application to Impurities, Surfaces, and Other Defects in Metals. *Phys. Rev. B* **1984**, *29*, 6443−6453.
(24) Deng, L.; Hu, W.; Deng, H.; Xiao, S.; Tang, J. Au−Ag Bimetallic Nanoparticles: Surface Segregation and Atomic-Scale Structure. *J. Phys. Chem. C* **2011**, *115*, 11355−11363.
(25) Shan, B.; Wang, L. G.; Yang, S.; Hyun, J.; Kapur, N.; Zhao, Y. J.; Nicholas, J. B.; Cho, K. First-Principles-Based Embedded Atom Method for PdAu Nanoparticles. *Phys. Rev. B* **2009**, *80*, 035404.
(26) Duan, Z.; Wang, G. Monte Carlo Simulation of Surface Segregation Phenomena in Extended and Nanoparticle Surfaces of Pt−Pd Alloys. *J. Phys.: Condens. Matter* **2011**, *23*, 475301.
(27) Deng, L.; Hu, W.; Deng, H.; Xiao, S. Surface Segregation and Structural Features of Bimetallic Au−Pt Nanoparticles. *J. Phys. Chem. C* **2010**, *114*, 11026−11032.
(28) Yuge, K. Segregation of $Pt_{28}Rh_{27}$ Bimetallic Nanoparticles: A First-Principles Study. *J. Phys.: Condens. Matter* **2010**, *22*, 245401.
(29) Ringe, E.; Van Duyne, R. P.; Marks, L. D. Wulff Construction for Alloy Nanoparticles. *Nano Lett.* **2011**, *11*, 3399−403.
(30) Wit, R. D. Partial Disclinations. *J. Phys. C* **1972**, *5*, 529.
(31) Howie, A.; Marks, L. D. Elastic Strains and the Energy-Balance for Multiply Twinned Particles. *Philos. Mag. A* **1984**, *49*, 95−109.
(32) Bagley, B. G. A Dense Packing of Hard Spheres with Five-Fold Symmetry. *Nature* **1965**, *208*, 674−675.
(33) Yang, C. Y. Crystallography of Decahedral and Icosahedral Particles: I. Geometry of Twinning. *J. Cryst. Growth* **1979**, *47*, 274−282.
(34) Ino, S. Stability of Multiply-Twinned Particles. *J. Phys. Soc. Jpn.* **1969**, *27*, 941−953.
(35) Volterra, V. Sur l'Équilibre des Corps Multiplement Connexes. *Annales Scientifiques de l'École Normale Supérieure* **1907**, *24*, 401.
(36) Marks, L. D. Surface-Structure and Energetics of Multiply Twinned Particles. *Philos. Mag. A* **1984**, *49*, 81−93.
(37) Patala, S.; Marks, L. D.; de la Cruz, M. O. Thermodynamic Analysis of Multiply Twinned Particles: Surface Stress Effects. *J. Phys. Chem. Lett.* **2013**, *4*, 3089−3094.
(38) Zhou, Y.; Fichthorn, K. A. Internal Stress-Induced Orthorhombic Phase in 5-Fold-Twinned Noble Metal Nanowires. *J. Phys. Chem. C* **2014**, *118*, 18746−18755.
(39) Cleveland, C. L.; Landman, U. The Energetics and Structure of Nickel Clusters — Size Dependence. *J. Chem. Phys.* **1991**, *94*, 7376−7396.
(40) Cottrell, A. H.; Bilby, B. A. Dislocation Theory of Yielding and Strain Ageing of Iron. *Proc. Phys. Soc., London, Sect. A* **1949**, *62*, 49−62.
(41) Wynblatt, P.; Chatain, D. Anisotropy of Segregation at Grain Boundaries and Surfaces. *Metall. Mater. Trans. A* **2006**, *37*, 2595−2620.
(42) Radwan, F. A. Some Properties of Copper−Gold and Silver−Gold Alloys at Different% of Gold. *Proceedings of the International MultiConference of Engineers and Computer Scientists*; Newswood Limited: Hong Kong, 2011.
(43) Liang, L.; Ma, H.; Wei, Y. Size-Dependent Elastic Modulus and Vibration Frequency of Nanocrystals. *J. Nanomater.* **2011**, *2011*, 6.
(44) Sasaki, K.; Naohara, H.; Choi, Y.; Cai, Y.; Chen, W. F.; Liu, P.; Adzic, R. R. Highly Stable Pt Monolayer on PdAu Nanoparticle Electrocatalysts for the Oxygen Reduction Reaction. *Nat. Commun.* **2012**, *3*, 1115.
(45) Lewis, E. A.; Slater, T. J.; Prestat, E.; Macedo, A.; O'Brien, P.; Camargo, P. H.; Haigh, S. J. Real-time Imaging and Elemental Mapping of AgAu Nanoparticle Transformations. *Nanoscale* **2014**, *6*, 13598−605.
(46) Pasini, T.; Piccinini, M.; Blosi, M.; Bonelli, R.; Albonetti, S.; Dimitratos, N.; Lopez-Sanchez, J. A.; Sankar, M.; He, Q.; Kiely, C. J.; Hutchings, G. J.; Cavani, F. Selective Oxidation of 5-Hydroxymethyl-2-furfural Using Supported Gold−Copper Nanoparticles. *Green Chem.* **2011**, *13*, 2091.
(47) Yin, A. X.; Min, X. Q.; Zhu, W.; Wu, H. S.; Zhang, Y. W.; Yan, C. H. Multiply Twinned Pt−Pd Nanoicosahedrons as Highly Active Electrocatalysts for Methanol Oxidation. *Chem. Commun.* **2012**, *48*, 543−5.
(48) Pohl, D.; Wiesenhutter, U.; Mohn, E.; Schultz, L.; Rellinghaus, B. Near-Surface Strain in Icosahedra of Binary Metallic Alloys: Segregational versus Intrinsic Effects. *Nano Lett.* **2014**, *14*, 1776−84.
(49) Wang, R. M.; Dmitrieva, O.; Farle, M.; Dumpich, G.; Ye, H. Q.; Poppa, H.; Kilaas, R.; Kisielowski, C. Layer Resolved Structural Relaxation at the Surface of Magnetic FePt Icosahedral Nanoparticles. *Phys. Rev. Lett.* **2008**, *100*, 017205.
(50) Li, Z. A.; Spasova, M.; Ramasse, Q. M.; Gruner, M. E.; Kisielowski, C.; Farle, M. Chemically Ordered Decahedral FePt Nanocrystals Observed by Electron Microscopy. *Phys. Rev. B* **2014**, *89*, 161406.
(51) Delalande, M.; Guinel, M. J. F.; Allard, L. F.; Delattre, A.; Le Bris, R.; Samson, Y.; Bayle-Guillemaud, P.; Reiss, P. $L1_0$ Ordering of Ultrasmall FePt Nanoparticles Revealed by TEM In Situ Annealing. *J. Phys. Chem. C* **2012**, *116*, 6866−6872.
(52) Gruner, M. E.; Rollmann, G.; Entel, P.; Farle, M. Multiply Twinned Morphologies of FePt and CoPt Nanoparticles. *Phys. Rev. Lett.* **2008**, *100*, 087203.
(53) Yang, B.; Asta, M.; Mryasov, O. N.; Klemmer, T. J.; Chantrell, R. W. Equilibrium Monte Carlo Simulations of A1−$L1_0$ ordering in FePt Nanoparticles. *Scr. Mater.* **2005**, *53*, 417−422.
(54) Müller, M.; Albe, K. Lattice Monte Carlo Simulations of FePt Nanoparticles: Influence of Size, Composition, and Surface Segregation on Order−Disorder Phenomena. *Phys. Rev. B* **2005**, *72*, 094203.
(55) Takahashi, Y. K.; Ohkubo, T.; Ohnuma, M.; Hono, K. Size Effect on the Ordering of FePt Granular Films. *J. Appl. Phys.* **2003**, *93*, 7166−7168.
(56) Chen, F.; Johnston, R. L. Charge Transfer Driven Surface Segregation of Gold Atoms in 13-Atom Au−Ag Nanoalloys and its Relevance to Their Structural, Optical and Electronic Properties. *Acta Mater.* **2008**, *56*, 2374−2380.
(57) Cerbelaud, M.; Ferrando, R.; Barcaro, G.; Fortunelli, A. Optimization of Chemical Ordering in AgAu Nanoalloys. *Phys. Chem. Chem. Phys.* **2011**, *13*, 10232−10240.
(58) Bochicchio, D.; Ferrando, R. Morphological Instability of Core−Shell Metallic Nanoparticles. *Phys. Rev. B* **2013**, *87*, 165435.
(59) Laasonen, K.; Panizon, E.; Bochicchio, D.; Ferrando, R. Competition between Icosahedral Motifs in AgCu, AgNi, and AgCo Nanoalloys: A Combined Atomistic−DFT Study. *J. Phys. Chem. C* **2013**, *117*, 26405−26413.
(60) Riccardo, F. Symmetry Breaking and Morphological Instabilities in Core−Shell Metallic Nanoparticles. *J. Phys.: Condens. Matter* **2015**, *27*, 013003.

DOI: 10.1021/acs.jpclett.5b00706
J. Phys. Chem. Lett. 2015, 6, 1930−1934